Dalton Transactions

Accepted Manuscript

This is an *Accepted Manuscript*, which has been through the RSC Publishing peer review process and has been accepted for publication.

Accepted Manuscripts are published online shortly after acceptance, which is prior to technical editing, formatting and proof reading. This free service from RSC Publishing allows authors to make their results available to the community, in citable form, before publication of the edited article. This *Accepted Manuscript* will be replaced by the edited and formatted *Advance Article* as soon as this is available.

To cite this manuscript please use its permanent Digital Object Identifier (DOI®), which is identical for all formats of publication.

More information about *Accepted Manuscripts* can be found in the **Information for Authors**.

Please note that technical editing may introduce minor changes to the text and/or graphics contained in the manuscript submitted by the author(s) which may alter content, and that the standard **Terms & Conditions** and the **ethical guidelines** that apply to the journal are still applicable. In no event shall the RSC be held responsible for any errors or omissions in these *Accepted Manuscript* manuscripts or any consequences arising from the use of any information contained in them.

View Online

Cite this: DOI: 10.1039/c0xx00000x

www.rsc.org/xxxxxx

ARTICLE TYPE

Ligand effect on the catalytic activity of ruthenium nanoparticles in ionic liquids

Gorka Salas,[a] Paul S. Campbell,[a] Catherine C. Santini,[a] Karine Philippot,[b] Margarida F. Costa Gomes,[c] Agílio A.H. Pádua[c]

Received (in XXX, XXX) Xth XXXXXXXXX 20XX, Accepted Xth XXXXXXXXX 20XX
DOI: 10.1039/b000000x

The authors wish to dedicate this paper to Professor David Cole-Hamilton in recognition of his significant contribution to homogeneous catalysis

Suspensions of small sized (1–2.5 nm) ruthenium nanoparticles (RuNPs) have been obtained by decomposition, under H_2, of (η^4-1,5-cyclooctadiene)(η^6-1,3,5-cyclooctatriene)ruthenium(0), [Ru(COD)(COT)], in the ionic liquid 1-butyl-3-methylimidazolium bis(trifluoromethylsulfonyl) imide, [C_1C_4Im][NTf_2], and in the presence of different compounds acting as ligands: $C_8H_{17}NH_2$, $PPhH_2$, PPh_2H and H_2O. Previous and new liquid NMR experiments showed that the ligands are coordinated or in the proximity to the surface of the RuNPs. Herein is reported how the ligand affects the catalytic performance (activity and selectivity) compared to a ligand-free system of RuNPs, when RuNPs in [C_1C_4Im][NTf_2] are used as catalysts for the hydrogenation of various unsaturated compounds (1,3-cyclohexadiene, limonene and styrene). It has been observed that σ-donor ligands increase the activity of the nanoparticles, contrarily to π-acceptor ones.

Introduction

Ionic liquids (ILs) are often termed as "*green solvents*" due to their low toxicity and low vapour pressure, and have been widely investigated as greener alternatives to conventional organic solvents aimed at facilitating sustainable chemistry. In addition to their "*green*" nature, ILs present many other interesting physico-chemical properties such as their high thermal stability, large *liquidus* range, high conductivities, large electrochemical window, and tuneable solubility and mixing properties. This has led to ever-growing interest for their use in diverse applications such as catalysis, separations, electrochemistry, etc.[1-4]

More interestingly, in recent years, ILs have been discovered to be excellent media in the controlled preparation and stabilisation of nano-structured materials.[5] For example, ILs have been successfully implemented as solvents and structure directing agents in the synthesis of novel mesoporous materials such as zeolites and silica aerogels,[6] the properties of the resulting materials being related directly back to the nature of the solvent used as well as the experimental conditions. Also, as recently extensively reviewed,[7,8] ILs are increasingly popular media for the generation and stabilisation of metallic nanoparticles (NPs), usually of the late transition metals, e.g. Pt, Pd, Au, Ag, Ru, etc. Here, ILs play a double role, acting both as solvent and as stabilizer, controlling the size of the NPs produced and preventing their aggregation.

The use of NPs as catalysts is a topic of growing interest at the frontier between homogeneous and heterogeneous catalysis.[9] As the activity and selectivity of metal NPs are dependent on their size and shape, it is of crucial importance to control these parameters.[10-13,14-16] Furthermore, an important factor in sustainable chemistry is the recyclability of catalysts. Under standard experimental catalytic conditions (temperature, stirring, or carbon monoxide atmosphere) ruthenium nanoparticles (RuNPs) in ILs have been found unstable towards agglomeration and coalescence, leading to gradual deactivation with each catalytic run.[17] Consequently, the addition of stabilising ligands is under development a strategy for enhanced NP stabilisation.[18] Therein, two different approaches have been reported: 1) The addition of a ligand such as bipyridine after the formation of NPs,[19, 20] 2) The incorporation of a coordinating moiety into the cation of the IL itself.[21-23]

In order to develop new catalytic systems based on stable and size-controlled NPs in ILs, recently, we have successfully combined the use of ILs and ligands to increase RuNP stability, the latter being present *during* the RuNP synthesis. This induces a highly recyclable catalytic system in toluene hydrogenation.[24] As the presence of appropriate ligands in traditional organic solvents can lead to selective catalysts,[16, 25] the question is as the ligand affects the catalytic performances (activity and selectivity) compared to a ligand-free system in ionic liquids.

Our group has reported that catalytic hydrogenation of cyclohexadiene (CYD) in ionic liquids is highly dependent on the physical-chemical parameters of the media, in particular the viscosity, which is in turn strongly dependent on the

concentration of substrate.[26, 27] Additionally, in tests maintaining constant parameters such as substrate/catalyst and substrate/ionic liquid ratio, and therefore viscosity and mass transport factors, we reported that the rate and product distribution of the same reaction catalysed by RuNPs in ILs varies with RuNP size. These results prove that the mass transport properties, the ionicity of the media and RuNP size play a crucial role and that these parameters must be vigorously controlled.[10, 28]

In the present work, we study the effect of various additional ligands on the catalytic behaviour of RuNPs synthesized in 1-butyl-3-methylimidazolium bis(trifluoromethylsulfonyl) imide, $[C_1C_4Im][NTf_2]$, compared to ligand-free RuNPs. The effect of the ligand on model hydrogenation reactions is investigated, whilst ensuring the parity of all important parameters, i.e. mass transport and RuNP size.

Experimental

Materials and Methods

All operations were performed in the strict absence of oxygen and water under a purified argon atmosphere using glovebox (Jacomex or MBraun) or vacuum-line Schlenk techniques. 1-octylamine (>99.5%, Fluka), phenylphosphine (Alfa Aesar) and diphenylphosphine (98%, Aldrich) were used without further purification. (η^4-1,5-cyclooctadiene)(η^6-1,3,5-cyclooctatriene) ruthenium(0), [Ru(COD)(COT)],[29] and $[C_1C_4Im][NTf_2]$, [30] were synthesised as reported. 1-Methylimidazole (>99%, Aldrich), chlorobutane (>99%, Aldrich), cyclohexadiene, styrene and (*R*)-(+)-limonene were distilled and stored under argon prior to use. Lithium bis(trifluoromethanesulfonyl)imide (Solvionic) was used without further purification.

Transmission electron microscopy (TEM) experiments were performed directly in the IL media. A thin film of RuNP suspension in IL was deposited on a carbon film supported by a copper grid. Conventional TEM micrographs were obtained at the Centre Technologique des Microstructures, Université Claude Bernard Lyon 1, Villeurbanne, France, using a Philips 120 CX electron microscope with acceleration voltage of 120 kV. Size distribution histograms were constructed from the measurement of at least 200 different NPs assuming a near spherical shape and random orientation.

Solution NMR spectra were recorded in a Bruker AV-300 spectrometer. ^{31}P spectra were referred internally to deuterated solvents; chemical shifts are relative to 85% H_3PO_4 (^{31}P).

Synthesis of the RuNPs.

RuNPs in $[C_1C_4Im][NTf_2]$ in the presence of 1-octylamine, phenylphosphine, diphenylphosphine or water were synthesized as previously described.[24]

Catalytic experiments

Each dispersion of RuNPs was produced from the decomposition of $4.2{\cdot}10^{-2}$ mol.L^{-1} of [Ru(COD)(COT)] in the IL as described.[10] Dispersions of RuNPs with different sizes have different concentrations of Ru atoms at the surface, [Ru_S]. Each dispersion was diluted with $[C_1C_4Im][NTf_2]$ to match a concentration [Ru_S] = $1.7{\cdot}10^{-2}$ mol.L^{-1}. For cyclohexadiene or styrene hydrogenation, 10 wt. % of substrate was used. Only 5 wt. % was used in the case of (R)-(+)-limonene, due to the lower solubility of this compound in $[C_1C_4Im][NTf_2]$. This gives catalytic mixtures with constant substrate/catalyst molar ratios of 105 (CYD), 175 (STY) and 65 (LIM), and constant substrate/IL molar ratios, ensuring identical viscosities and a single phase. From dispersions prepared as described, aliquots of 0.5 mL were transferred to identical Schlenk tubes containing cross-shaped magnetic stirrer bars. After 30 min, when the temperature had stabilized, the Schlenk tubes were charged with 1.2 bar of H_2 and kept at constant pressure and temperature during the time of the reaction. The solubility of the reaction products is lower than those of the starting compounds, therefore the medium may tend to a biphasic system during the course of the reaction. For this reason, each reaction time corresponds to a single experiment in which, after *t* minutes (e. g. 5, 10, 20, 30, 45, 60, 90 and 120), the Schlenk tube was isolated and opened to air, quenching the reaction with 10 mL of a 1 M solution of toluene in acetonitrile. In this way, the reaction mixture was entirely dissolved. The distribution of products in the reaction mixture and the conversion were determined by GC analyses using a HP6890 chromatograph equipped with a FID detector and a cross-linked methyl siloxane column (L = 30 m, D_{int} = 0.32 mm, film thickness = 0.25 µm). Toluene was used as internal standard. The injector and detector temperatures were both set to 230°C. Samples were injected in volumes of 1 µL. The temperature of the column was fixed at 70°C for 13.5 min, followed by a temperature ramp of 40°C min-1 up to 250°C.

Results and Discussion

The size of RuNPs in 1-butyl-3-methylimidazolium bis(trifluoromethylsulfonyl)imide, $[C_1C_4Im][NTf_2]$, prepared by decomposition of (η^4-1,5-cyclooctadiene)(η^6-1,3,5-cycloocta -triene)ruthenium(0) [Ru(COD)(COT)] with dihydrogen (3 bar) can be controlled by varying experimental conditions. When the decomposition is carried out at 0 ºC these RuNPs display an average diameter of 1.1 nm, whereas at 25 ºC, 2.3 nm RuNPs are formed.[10, 31] This decomposition run at 25 °C in the presence of $C_8H_{17}NH_2$ (octylamine; OA) as ligand, with a molar ratio [OA]/[Ru(COD)(COT)] *r* = 0.2, gives a stable suspension of small sized (1.1 nm) and homogeneously dispersed RuNPs, no matter the IL used.[24] Interestingly, when OA is added in the same ratio to a suspension of ligand-free 1.1 nm RuNPs in IL, flocculation occurs leading to large agglomerates of RuNPs.[32] As such agglomeration may lead to less available metal surface for catalysis, this study focuses only on RuNPs directly produced in the presence of ligand.

Therefore, in the present work, the decomposition of [Ru(COD)(COT)] with dihydrogen was carried out at 30°C *in the presence* of different ligands (L) in order to study the effect of [L]/[Ru] ratio, and electronic and steric properties of these ligands on the resulting NP size, stabilisation against coalescence and on the catalytic activity. For this purpose, ligands namely, octylamine (OA), water (L1), phenylphosphine (L2), and diphenylphosphine (L3), scheme 1, presenting different heteroatoms (N, P, O), and steric hindrance (i.e. L2 vs. L3) have been selected. In all experiments, total decomposition of [Ru(COD)(COT)] into RuNPs is verified by GC quantification of the cyclooctane resulting from the hydrogenation of COD and COT ligands.

View Online

Cite this: DOI: 10.1039/c0xx00000x

www.rsc.org/xxxxxx

ARTICLE TYPE

Table 1 Data summary of the RuNPs obtained in $[C_1C_4Im]][NTf_2]$, depending on the ratio r = [L]/[Ru(COD)(COT)]. L = octylamine (OA), phenylphosphine (L2), diphenylphosphine (L2) or water (L1). Reaction temperature = 0 °C (entry 1),[31] 25 °C (entry 2),[31] 30 °C (entries 3-9). Reaction time = 20 h (entries 2 and 3) or 3 days (entries 1, 5 and 6).

Entry	L	r	Average diameter (nm) [(a)]	$[Ru_S]$ (10^{-2} M)[(b)]	$[Ru_S]/[Ru_T]$[(c)]	$[L]/[Ru_S]$[(d)]	Label
1	–	0	1.1 (0.2)	3.4	0.81	–	Ru^0
2	–	0	2.3 (0.3)	2.1	0.51	–	Ru^{25}
3	$C_8H_{17}NH_2$	0.1	1.6 (0.5)	2.7	0.64	0.16	$Ru_{OA0.1}$
4	$C_8H_{17}NH_2$	0.2	1.1 (0.3)	3.4	0.81	0.25	$Ru_{OA0.2}$
5	$C_8H_{17}NH_2$	0.5	1.0 (0.3)	3.6	0.86	0.60	$Ru_{OA0.5}$
6	$C_8H_{17}NH_2$	1.0	1.0 (0.3)	3.6	0.86	1.2	Ru_{OA1}
7	H_2O	0.2	2.5 (0.7)	2.0	0.48	0.52	Ru_{L1}
8	$PPhH_2$	0.2	2.2 (0.6)	2.2	0.52	0.38	Ru_{L2}
9	PPh_2H	0.2	2.2 (0.5)	2.2	0.52	0.38	Ru_{L3}

(a) Measured from TEM micrographs, standard deviation is indicated in brackets. (b) concentration of Ru(COD)(COT) (c) Dispersion: ratio between surface Ru atoms (Ru_S) and the total number of Ru atoms in the nanoparticles (Ru_T).10 (d) Ratio between the total concentration of ligand and the concentration of Ru atoms at the surface (Ru_S) .

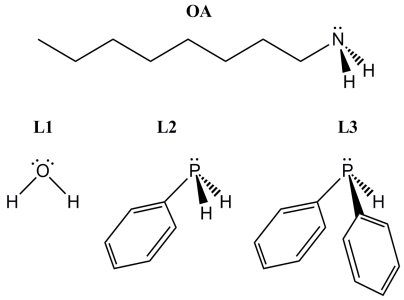

Scheme 1 The ligands under study: 1-octylamine (OA), water (L1), phenylphosphine (L2), diphenylphosphine (L3).

Synthesis of RuNPs in $[C_1C_4Im][NTf_2]$ in the presence of L

Influence of L/Ru ratio

The reaction carried out at 30 ºC in the presence of different molar ratios of octylamine [OA]/[Ru(COD)(COT)] r = 0; 0.1; 0.2; 0.5 and 1, affords small RuNPs with narrow size distributions. [24] These RuNPs are well dispersed, almost spherical, and stable for months (stored at room temperature under argon). High resolution electron microscopy (HREM) has been already used to verify the crystalline nature of the RuNPs formed.[24] With the exception of r = 0.1, where RuNPs with a diameter of 1.6 nm were obtained (Table 1), small RuNPs displaying a mean diameter around 1 nm are observed. Interestingly, ligand-free RuNPs synthesised under the same conditions display a mean diameter of 2.3 nm and only by lowering the reaction temperature to 0°C can RuNPs of around 1 nm be obtained.[31] However, RuNPs prepared in THF with 0.2 molar equivalents of OA display a mean size of 2.3 nm but are agglomerated in large superstructures (100 nm).[33] This clearly indicates a better stabilisation when combining ligands with ILs.

In the presence of OA a beneficial synergic effect is observed in the formation of RuNPs in $[C_1C_4Im][NTf_2]$, which we have already attempted to rationalise through NMR studies of the interaction between RuNPs and OA in IL. Indeed, previous ^{13}C NMR and ^1H DOSY NMR results have proven the coordination of the amine to the ruthenium through the amino group.[32]

However, following the r value, these ^{13}C NMR experiments suggest a different organisation of OA around the RuNPs as depicted in Fig. 1. Here, at low values of r the long alkyl chains of the OA are found lying on the RuNP surface, whereas at high values of r, they are pointing away from the surface of the NP. This behaviour is supported by the close proximity of the methyl group of the alkylchain to the metal surface as observed by NMR at low concentration of OA. Furthermore, both ^1H DOSY NMR

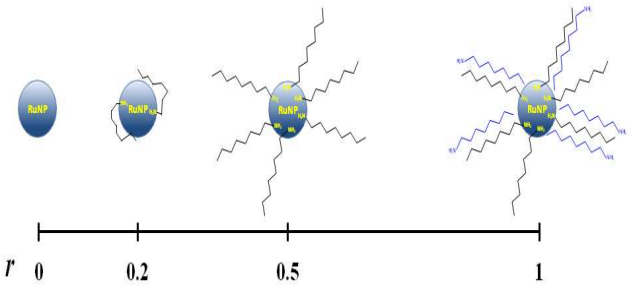

Fig.1 Cartoon illustrating the coordination of OA to RuNPs and the association between OA molecules at high OA concentration.

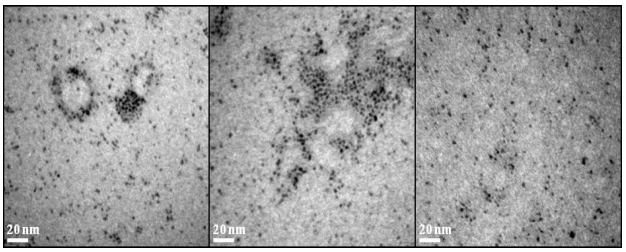

Fig. 2 Selected TEM micrographs of Ru_{L1} (L1 = H_2O); Ru_{L2} (L2 = $PPhH_2$) and Ru_{L3} (L3 = PPh_2H)

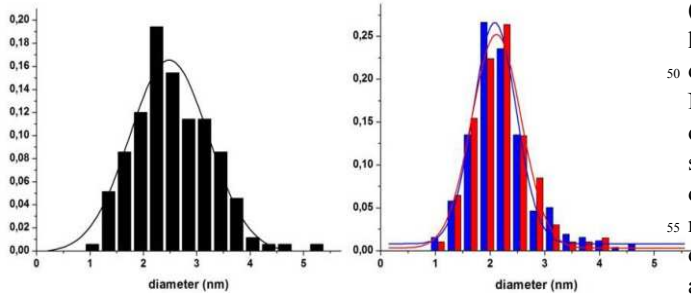

Fig. 3 Normalized size distribution histograms of Ru_{L1} (L1 = H_2O, left), Ru_{L2}, (L2 = $PPhH_2$, right in blue) and Ru_{L3} (L3 = PPh_2H, right in red).

experiments and calorimetric measurements also showed that in addition to the OA-RuNP coordination, for r = [OA]/[Ru(COD)(COT)] = 1 (Ru_1), there exists also some degree of association between OA molecules (Fig. 1), a finding also corroborated by molecular simulation.[32]

The larger nanoparticle diameter obtained for r = 0.1 and the subsequent identical nanoparticle diameters obtained for 0.2 < r < 1.0 suggest that above r = 0.2 the number of OA ligands coordinated at the surface attains a threshold that inhibits further growth of the nanoparticles.

Influence of the nature of the ligand

The synthesis of RuNPs in $[C_1C_4Im][NTf_2]$ in the presence of H_2O (L1), $PPhH_2$ (L2) and PPh_2H (L3), with r = 0.2, was performed under identical conditions than with OA. All these RuNPs display sizes over 2 nm (Table 1, entries 7–9; see also TEM micrographs in Fig. 2). In addition, the size distribution with these ligands is broader than in the case with OA (Fig. 3 and Table 1).

Examination of the suspensions of Ru_{L2} and Ru_{L3} in $[C_1C_4Im][NTf_2]$ by ^{31}P NMR spectroscopy, leads to no observed signal, probably due to a large broadening of the signals due to the fast spin-spin relaxation of the phosphorous atoms close to the nanoparticles, or signals because of a fast spin-spin relaxation of anisotropic chemical and Knight shifts, that make P signals unobservable.[34] However, when hydrogen peroxide is added to Ru_{L2}, one signal at 40 ppm arises in the ^{31}P NMR spectrum. This is due to the oxidation of the phosphine ligand and release of partially or fully oxidized phosphine in the solution making it observable, in agreement with previous reports in the literature.[35] The addition of hydrogen

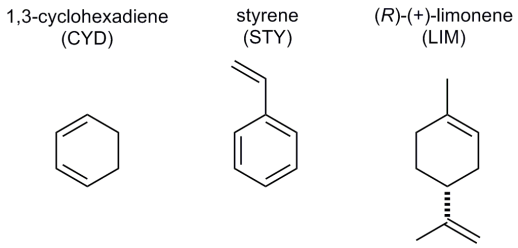

Scheme 2 Unsaturated substrates studied in this work.

peroxide to Ru_{L3} gives rise to three signals (40, 39, 23 ppm) instead of one. RuNPs in the presence of H_2 are known catalysts in the hydrogenation of aromatic compounds,[24] so partial or total hydrogenation of the initial phosphine can occur during the synthesis, producing a mixture of PPh_2H, PCyPhH and PCy_2H (Cy = cyclohexyl).[36] Indeed, we have already shown that the hydrogenation of aromatic ring occurs during the decomposition of Ru(COD)(COT) even at 0 °C.[17] The observed signals in the ^{31}P NMR spectrum, after hydrogen peroxide addition, correspond to oxidation products of the three phosphines. With Ru_{L2} the single signal observed after oxidation is most probably due to the oxidation product of $PCyH_2$. It is difficult to predict the exact nature of the products of the phosphines after hydrogenation and oxidation (with the hydrogen peroxide) in the presence of RuNPs and under the conditions described in this work. Different compounds as phosphine oxides, phosphonates, phosphinic acids and related compounds could have been formed, without discarding that in addition those compounds may undergo other reactions as P-C cleavage. Attempts to characterize the nature of the hydrogenation/oxidation of the phosphines by mass spectrometry were unsuccessful. Nevertheless, the chemical shifts of 40 and 39 ppm are close to that described for cyclohexylphosphinic acid (41.9 ppm), and in the range of other reported for alkyl-, dialkyl- and alkylarylphosphinic acids and phosphinates.[37, 38]

Catalytic hydrogenation of unsaturated compounds

The former results suggest that the ligands added to increase the stability of the RuNPs are coordinated or in close proximity to the metal surface. Therefore, the effect of these ligands on the catalytic behaviour of RuNPs synthesized in 1-butyl-3-methylimidazolium bis(trifluoromethylsulfonyl) imide, $[C_1C_4Im][NTf_2]$ compared to ligand-free RuNPs can be investigated, ensuring the parity of all important parameters, i.e. mass transport and RuNP size.

The catalytic performances of the systems described above was tested in the hydrogenation of model unsaturated substrates (Scheme 2): 1,3-cyclohexadiene (CYD), styrene (STY) and R-(+)-limonene (LIM). These substrates have more than one unsaturation in their structure, so the activity and the selectivity

can be examined.

In the present work, all experiments were carried out at 30 ºC under a H_2 pressure of 1.2 bar. The **substrate/Ru$_S$** (Ru_S: Ru atoms at the surface of the nanoparticle) ratio and **substrate/IL** ratio were kept constant but adapted to each substrate (see details in Experimental Part), ensuring that the concentration of substrate was kept below its solubility limit to prevent formation of a biphasic mixture. Consequently, for CYD and for STY substrate-to-IL mass ratios of 10 wt. % were used, affording the molar ratios of **CYD/Ru$_S$** and of **STY/Ru$_S$** equal to 105 and 175, respectively. The concentration of LIM, which presents a lower solubility in $[C_1C_4Im][NTf_2]$, was 5 wt.% giving a molar ratio **LIM/Ru$_S$** of 65%.

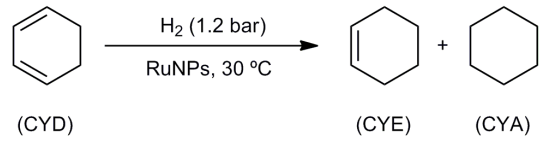

Scheme 3 Reaction products of the hydrogenation of 1,3-cyclohexadiene.

The different dispersion values (**D = Ru$_S$/Ru$_T$**; Ru_T: total amount of Ru atoms) must also be taken into account for each size of NPs formed in order to maintain constant the initial ratio of substrate to Ru_s. Moreover, all the reaction mixtures were prepared by dilution of the colloids with different volumes of $[C_1C_4Im][NTf_2]$, to ensure identical concentrations of $[Ru_S]$ = $1.7 \cdot 10^{-2}$ M (see Experimental Part).

Finally, as the colloidal size has been proven to play an important role,[10] and due to the differences in size observed depending on the nature of the ligand (Table 1), we have divided the colloidal systems in two sets of catalysts to compare them independently. The first set corresponds to RuNPs with sizes around 1 nm: Ru^0, $Ru_{OA0.2}$, $Ru_{OA0.5}$ and Ru_{OA1} (Ru^0 = RuNPs generated in absence of ligand at 0 °C, as previously described[31]). The second set comprises all RuNPs with sizes around 2.2 nm:, Ru^{25}, Ru_{L1}, Ru_{L2} and Ru_{L3} (Ru^{25} = RuNPs generated in absence of ligand at 25°C, as previously described[31]). Due to its different size compared to other systems, the catalytic behaviour of $Ru_{OA0.1}$ is not discussed herein.

Catalytic hydrogenation of 1,3-cyclohexadiene

The hydrogenation reaction of CYD can afford two different products: the partial hydrogenation product, cyclohexene (CYE), and the full hydrogenation product, cyclohexane (CYA) (Scheme 3). In IL media, it has already been reported that CYD can be partially hydrogenated with high selectivity by molecular catalysts.[39-41]

In previous work from our group, hydrogenation of CYD was performed with tailor-made, size-controlled and ligand free RuNPs (1 to 3 nm).[10] It was found that the activity increases with the NP size in agreement with the literature results on heterogeneous catalysts.[12, 15, 42] Contrarily to activity, the selectivity for CYE versus CYA drops from 97% to 80% when the RuNP size increases from 1.1 to 2.9 nm. These results were in agreement with a mechanism involving π-bond activation and double coordination of diene-substrates, necessitating several neighbouring surface atoms only found in facial positions on the larger NPs.[43, 44]

RuNPs with a mean size of 1.1 nm

The conversion of CYD *vs.* time with Ru^0, $Ru_{OA0.2}$, $Ru_{OA0.5}$ and Ru_{OA1} is represented in Fig. 4. When the amine is coordinated to the nanoparticle it is hindering access to catalytically active sites so, in principle a predictable result would be a decrease in the catalyst activity. Nevertheless the reaction proceeds unexpectedly faster with $Ru_{OA0.2}$ compared to Ru^0. On the other hand, with $Ru_{OA0.5}$ and Ru_{OA1} where the ratio OA per **Ru$_S$** is 0.6 and 1.2, respectively, the steric hindrance becomes more important, and the reaction is therefore slowed compared to $Ru_{OA0.2}$.

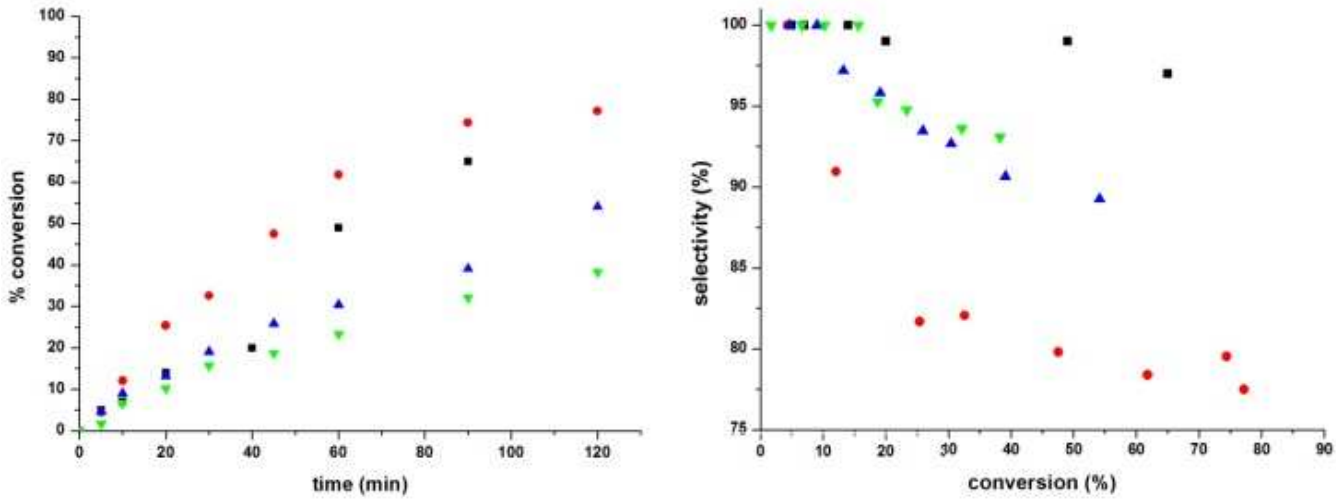

Fig. 4 Left: Conversion (%) of CYD, into CYE and CYA with time in the presence of RuNPs of around 1.1 nm. Right: Selectivity (100·[CYE] / CYE] + [CYA])) as a function of conversion in CYD hydrogenation (note that the *y* axe is truncated). Ru^0 (■), $Ru_{OA0.2}$ (●), $Ru_{OA0.5}$ (▲), Ru_{OA1} (▼). (Ru^0: NPs generated in absence of ligand at 0 °C).[31]

View Online

Cite this: DOI: 10.1039/c0xx00000x

www.rsc.org/xxxxxx

ARTICLE TYPE

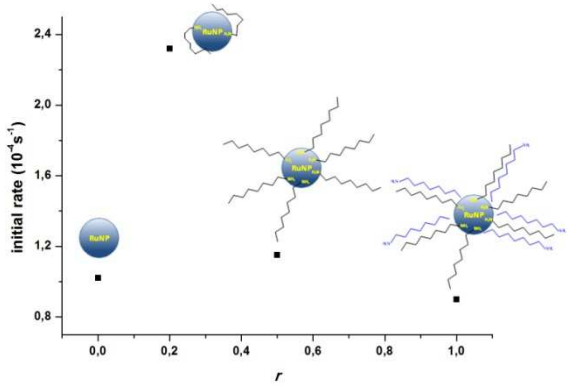

Fig. 5 Initial rates in the catalytic hydrogenation of CYD with RuNPs synthesized in the presence of different amounts of octylamine. [a] Calculated from the first points of the $[CYD]/[CYD]_0$ variation versus time ($[CYD]_0$ = initial concentration of CYD).

Note that for the OA ligand when the ratio L /Ru_S increases from 0.2 to 1 the activity decreases sharply (Fig. 5). Considering that to undergo hydrogenation, the olefin needs to be coordinated to the NP surface, the presence of ligands will reduce the number potentially active molecular species that could be stabilized by octylamine. This would eventually enhance the reaction activity of the system. If this was the case, then an excess of octylamine directly added to the RuNPs synthesized without any ligand, Ru^0, should provide a more active system than Ru^0 itself. We have verified this possibility using mixtures of Ru^0 and octylamine with molar ratios (r) OA/Ru_T = 0.2 and 0.5, prepared as previously described.[24] The hydrogenation of CYD with these mixtures as catalysts affords conversions of 38 % and 20 % after 90 minutes, in contrast to the 65 % observed with Ru^0. The lower activities observed in the systems with octylamine added after RuNP synthesis indicate that the potential formation of ruthenium molecular species, and their subsequent stabilization by octylamine, does not play a role in the enhanced activity observed for $Ru_{OA0.2}$ and $Ru_{OA0.5}$.

One plausible explanation of these results is to consider both the electronic and steric effects of the ligands. The hydrogenation of an unsaturated compound is a reduction. Thus if the ligand

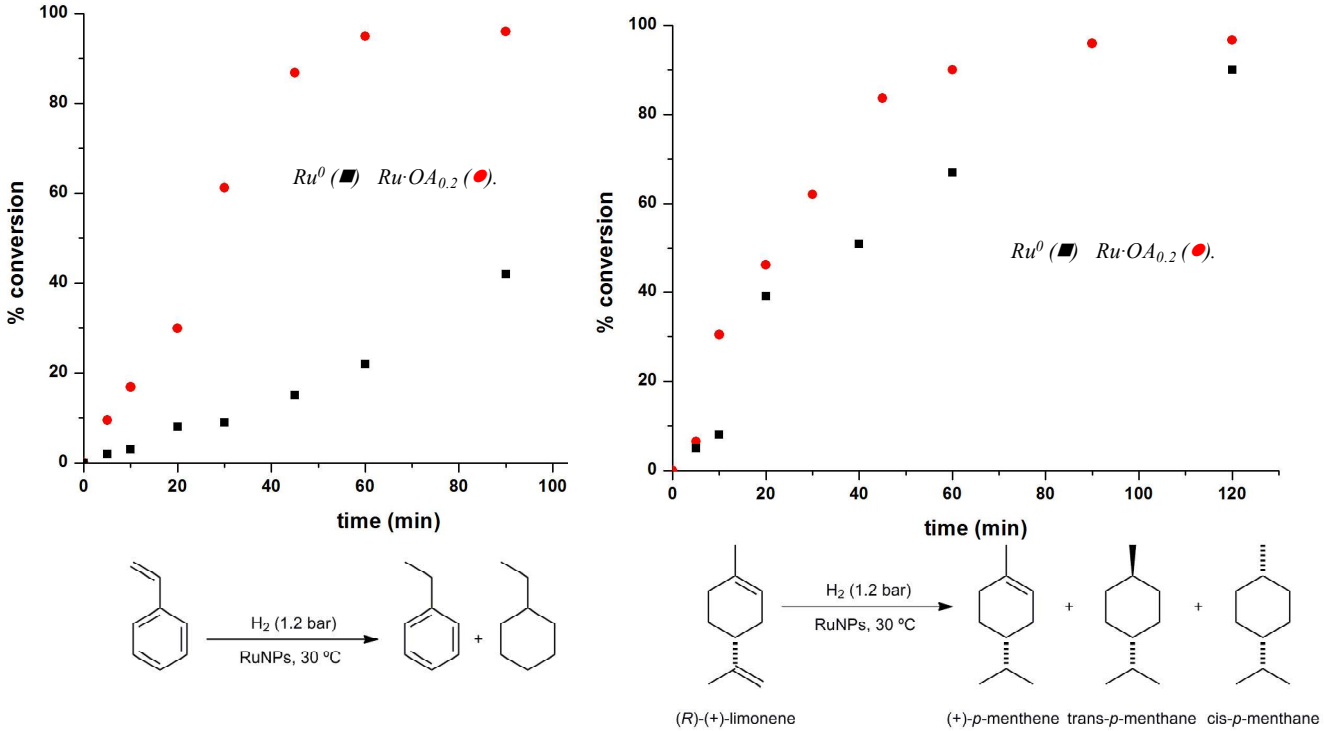

Fig. 6 Left: Progress of the conversion (%) of STY with time. Ru^0 (■), $Ru_{OA0.2}$ (●). Reaction scheme with possible products ethylbenzene and ethylcyclohexane depicted below. Right: Progress of the conversion of LIM into menthene and menthane with time. Ru^0 (■), $Ru_{OA0.2}$ (●).

effect, the expected result is a lower catalytic performance with increasing amounts of octylamine.

To explain these results, one hypothesis that has been considered, and discarded, is Ru leaching into the IL forming increases the electronic density of the catalyst, then the reaction can be favoured. More thoroughly, the bonding of the double bond to the metal surface can be described by the Dewar-Chatt-Duncanson model: σ-donation of the olefin to the metal and π-

back donation from the metal to the empty π* orbital of the olefin, partially lowering the order of the C=C double bond (rehybridization). It can be hypothesized that the amine, a σ-donor ligand, coordinated to the RuNPs increases the electron density at the surface of the NP, favouring the π-back donation from the *d* orbitals of the metal to the antibonding π* orbital of the olefin, and consequently facilitating its hydrogenation. Assuming this, when increasing the amount of amine at the surface of the NPs, both electron density and steric hindrance increase. The former effect favours the catalytic reaction, while the latter inhibits it. From the results obtained in this work we can conclude that, in $Ru_{OA0.2}$, steric hindrance is not important enough to inhibit the reaction, and the electronic effect predominates, accelerating the reaction. At higher quantity of OA ($Ru_{OA0.5}$ and Ru_{OA1}), the steric effects predominate and limit the reaction.

In order to generalise this result, we have also compared Ru^0 and $Ru_{OA0.2}$ in the hydrogenation of STY and of LIM. With STY the only detectable compound in the reaction was ethylbenzene (Fig. 6 left). It has been largely reported that arene hydrogenation at room temperature is slow with these systems probably due to the small NP size.[43, 44] The profile of conversion *vs.* time shows to the low solubility of the hydrogenation product in the IL solvent. Although the overall concentration of OA in the IL is too low to give a measurable effect on the macroscopic solubility of CYE, the presence of OA ligands at the NP surface leads to a stabilization of CYE near the NP (and thus near the coordination sphere of Ru) and favours a further step of hydrogenation.[27]

RuNPs with a mean size of 2.2 nm

The reaction proceeds faster with Ru_{L1} compared to Ru^{25}. This could be explained by a sigma donation of L1 ligand. However Ru_{L1} *NPs* are slightly larger than for Ru^{25} (Table 1), which can also account for the higher activity observed.[10]

On the other hand, Ru_{L2} and Ru_{L3} display similar activities and are less active than Ru^{25}. This cannot be attributed solely to steric hindrance since both systems present identical activities, despite the differing bulk of the two stabilising ligands. Probably, the σ-donor and π-acceptor properties of these ligands play a role, as recently proposed in the hydrogenation of methylanisole in the presence of RuNPs coordinated to diphosphine ligands.[36] Indeed, phosphines through π-back bonding may decrease the electron density on the metal surface. The π-back bonding capability of the metal, from the *d* orbitals of the metal, to the antibonding π* orbital of the olefin would be therefore reduced in turn, decreasing the rate of hydrogenation. Note that in the presence of L = CO, a strong π-acceptor, such RuNPs are rendered inactive in olefin hydrogenation.[17]

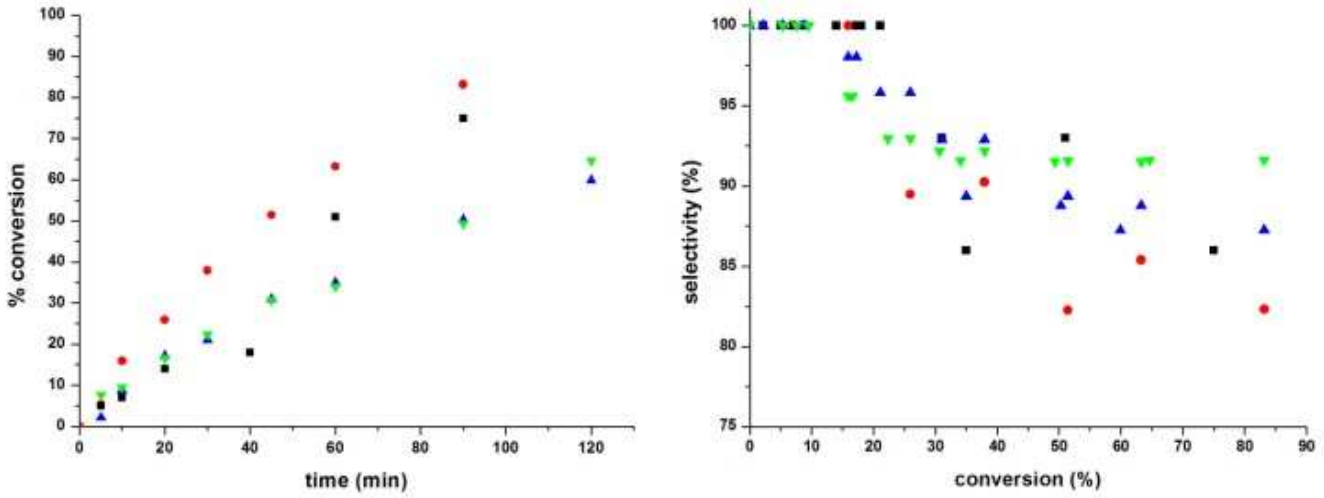

Fig. 7 Left: Progress of the conversion (%) of CYD, into CYE and CYA with time in the presence of RuNPs of around 2.2 nm. Right: Selectivity (100·[CYE] / ([CYE] + [CYA])) as a function of conversion in CYD hydrogenation (note that the *y* axe is truncated) Ru^{25} (■), Ru_{L1} (●), Ru_{L2} (▲), Ru_{L3} (▼) (Ru^{25} = NPs generated in absence of ligand at 25 °C,[31] L_1 = water, L_2 = phenylphosphine, L_3 = diphenylphosphine).

the same unexpected trend as with CYD albeit more pronounced; $Ru_{OA0.2}$ is much more active than Ru^0. This highlights the beneficial effect of the amine. Among the different potential products of the hydrogenation of LIM, only menthene and sphere of Ru) and favours a further step of hydrogenation.[27]

menthane were observed (Fig. 6 right). Menthane was observed as 50:50 mixtures of *cis* and *trans* isomers. Yet again, the hydrogenation proceeds faster with $Ru_{OA0.2}$ than with Ru^0.

Contrarily to activity, in the CYD hydrogenation, the selectivity in CYE versus CYA decreases sharply from in the presence of OA, notably from 97% (Ru^0) to 75% ($Ru_{OA0.2}$). The decrease of selectivity in the presence of OA is compatible with a

Conclusion

In this work the catalytic hydrogenation of 1,3-CYD, STY and LIM**,** in the IL $[C_1C_4Im][NTf_2]$ were used as probe reactions to study the effect of different ligands on the catalytic performances of RuNPs. Firstly, tailor-made, size-controlled and zero-valent RuNPs (1 to 2.3 nm) were generated from the decomposition of [Ru(COD)(COT)] under H_2 in $[C_1C_4Im][NTf_2]$, in the presence and absence of various ligands: $C_8H_{17}NH_2$, H_2O, $PPhH_2$ and PPh_2H. The mean size of these RuNPs was determined *in situ* by TEM. The coordination of the ligands or their close proximity to

the metal surface was evidenced by NMR experiments. Secondly, in carefully controlled catalytic tests, it was found that for hydrogenations of 1,3-CYD, STY and LIM the activity of the RuNP catalysts increases with σ-donor ligands such as 1-$C_8H_{17}NH_2$ and H_2O, but decreases with the bulkier and π-acceptor ligands, $PPhH_2$ PPh_2H and CO. These results underline the pseudo-molecular nature of NPs with sizes under 3 nm since their activity can be controlled following the σ-π-ligand character as with a homogeneous catalyst.

Acknowledgements

P. S. C. acknowledges the Ph.D. grant attributed by the *Ministère de l'Enseignement Supérieur et de la Recherche*, France and the EU transnational access programme. G. S. thanks the post-doctoral financial support by the project ANR CALIST. This work has been funded by CNRS and ANR (ANR project CALIST, ANR-07-CP2D-02-03).

Inserting Graphics

Use the buttons on the graphics dialog (accessed from the main toolbar by pressing the "Insert Graphics" button) to insert the required template text. It is recommended that graphics are inserted once the text is completed, as the text after graphic insertion will cause the graphics to move unpredicatably. Graphics should be inserted at the top of the page where they are first mentioned (unless they are equations, which appear in the flow of the text). Place the cursor at the beginning of the first line in either of the columns and press the required button.

Notes and references

[a] *Université de Lyon, Institut de Chimie de Lyon, UMR 5265 CNRS-Université de Lyon 1-ESCPE Lyon,C2P2, Equipe Chimie Organométallique de Surface, 43 bd du 11 Novembre 1918, 69626 Villeurbanne Cedex, France. Fax: +33 472431795; Tel: +33 472431794; E-mail: catherine.santini@univ-lyon1.fr* [b] *Laboratoire de Chimie de Coordination; CNRS; LCC; 205 Route de Narbonne, F-31077 Toulouse, France; Université de Toulouse; UPS, INPT; LCC; F-31077 Toulouse, France*[c] *(Institut de Chimie de Clermont-Ferrand, Université Blaise Pascal Clermont-Ferrand & CNRS, BP 80026, 63171 Aubière, France)*

1. H. Olivier-Bourbigou, L. Magna and D. Morvan, *Appl. Catal., A*, 2010, **373**, 1-56.
2. P. Wasserscheid and T. Welton, *Ionic liquids in synthesis*, Wiley-VCH, Weinheim, 2008.
3. F. Endres, D. MacFarlane and A. P. Abbott, *Electrodeposition from Ionic Liquids*, Wiley-VCH, Weinheim, 2008.
4. K. E. Ohno, *Electrochemical Aspects of Ionic Liquids*, Wiley-VCH, Tokyo, 2004.
5. T. Torimoto, T. Tsuda, K.-i. Okazaki and S. Kuwabata, *Adv. Mater.* , 2010, **22**, 1196-1221.
6. M. Antonietti, D. Kuang, B. Smarsly and Y. Zhou, *Angew. Chem. Int. Ed.*, 2004, **43**, 4988-4992.
7. J. Dupont and J. D. Scholten, *Chem. Soc. Rev.*, 2010, **39**, 1780-1804.
8. A. Gual, C. Godard, S. Castillon, D. Curulla-Ferre and C. Claver, *Catalysis Today*, 2012, **183**, 154-171.
9. D. Astruc, *Nanoparticles and Catalysis*, Wiley-VCH, Weinheim, 2008.
10. P. S. Campbell, C. C. Santini, F. Bayard, Y. Chauvin, V. Colliere, A. Podgorsek, G. M. F. Costa and J. Sa, *J. Catal.*, 2010, **275**, 99-107.
11. D. Uzio and G. Berhault, *Catal. Rev.*, 2010, **52**, 106-131.
12. P. J. Ellis, I. J. S. Fairlamb, S. F. J. Hackett, K. Wilson and A. F. Lee, *Angew. Chem. Int. Ed.* , 2010, **49**, 1820-1824.
13. K. Lee, M. Kim and H. Kim, *J. Mat. Chem.*, 2010, **20**, 3791-3798.
14. A. Z. Moshfegh, *J. Phys. D: Apply. Phys.*, 2009, **42**, 233001(233032pp.).
15. G. A. Somorjai and J. Y. Park, *Top Catal.*, 2008, **49**, 126-135.
16. A. Roucoux, A. Nowicki and K. Philippot, in *Nanoparticles*, ed. D. Astruc, Wiley-VCH, Weinheim, 2007, pp. 349-388.
17. P. S. Campbell, C. C. Santini, D. Bouchu, B. Fenet, K. Philippot, B. Chaudret, A. A. H. Padua and Y. Chauvin, *Phys. Chem. Chem. Phys.*, 2010, **12**, 4217-4223.
18. J. D. Scholten, B. C. Leal and J. Dupont, *ACS Catal.*, 2012, **2**, 184-200.
19. B. Leger, A. Denicourt-Nowicki, H. Olivier-Bourbigou and A. Roucoux, *ChemSusChem*, 2008, **1**, 984-987.
20. B. Leger, A. Denicourt-Nowicki, H. Olivier-Bourbigou and A. Roucoux, *Inorg. Chem.*, 2008, **47**, 9090-9096.
21. M. Crespo-Quesada, R. R. Dykeman, G. Laurenczy, P. J. Dyson and L. Kiwi-Minsker, *Journal of Catalysis*, 2011, **279**, 66-74.
22. R. R. Dykeman, N. Yan, R. Scopelliti and P. J. Dyson, *Inorganic Chemistry*, 2011, **50**, 717-719.
23. M. H. G. Prechtl, J. D. Scholten and J. Dupont, *J. Mol. Catal. A.*,, 2009, **313**, 74-78.
24. G. Salas, C. Santini Catherine, K. Philippot, V. Colliere, B. Chaudret, B. Fenet and F. Fazzini Pier, *Dalton. Trans.* , 2011, **40**, 4660-4668.
25. I. Favier, E. Teuma and M. Gomez, *C. R. Chimie*, 2009, **12**, 533-545.
26. P. S. Campbell, A. Podgorsek, T. Gutel, C. C. Santini, A. A. H. Padua, G. M. F. Costa, F. Bayard, B. Fenet and Y. Chauvin, *J. Phys. Chem. B*, 2010, **114**, 8156-8165.
27. A. Podgorsek, G. Salas, P. S. Campbell, C. C. Santini, A. A. H. Padua, G. M. F. Costa, B. Fenet and Y. Chauvin, *J. Phys. Chem. B*, 2011, **115**, 12150-12159.
28. K. L. Luska and A. Moores, *Green Chem.*, 2012, **14**, 1736-1742.
29. P. Pertici, G. Vitulli, M. Paci and L. Porri, *Dalton Trans.*, 1980, 1961-1964.
30. L. Magna, Y. Chauvin, G. P. Niccolai and J.-M. Basset, *Organometallics*, 2003, **22**, 4418-4425.
31. T. Gutel, J. Garcia-Anton, K. Pelzer, K. Philippot, C. C. Santini, Y. Chauvin, B. Chaudret and J.-M. Basset, *J. Mater. Chem.*, 2007, **17**, 3290-3292.
32. G. Salas, A. Podgorsek, P. S. Campbell, C. C. Santini, A. A. H. Padua, G. M. F. Costa, K. Philippot, B. Chaudret and M. Turmine, *Phys. Chem. Chem. Phys.*, 2011, **13**, 13527-13536.
33. C. Pan, K. Pelzer, K. Philippot, B. Chaudret, F. Dassenoy, P. Lecante and M.-J. Casanove, *J. Am. Chem. Soc.*, 2001, **123**, 7584-7593.
34. C. P. Slichter, *Principles of Magnetic Resonance*, Springer, New York, 1990.
35. J. Garcia-Anton, M. R. Axet, S. Jansat, K. Philippot, B. Chaudret, T. Pery, G. Buntkowsky and H.-H. Limbach, *Angew. Chem. Int. Ed.*, 2008, **47**, 2074-2078.

36. D. Gonzalez-Galvez, P. Nolis, K. Philippot, B. Chaudret and P. W. N. M. van Leeuwen, *Acs Catalysis*, 2012, **2**, 317-321.
37. S. Deprele and J. L. Montchamp, *J. Org. Chem.*, 2001, **66**, 6745-6755.
38. C. Petit, F. Fecourt and J.-L. Montchamp, *Adv. Synth. Catal.*, 2011, **353**, 1883-1888.
39. Y. Chauvin, L. Mussmann and H. Olivier-Bourbigou, *Angew. Chem. Int. Ed.*, 1995, **34**, 2698-2700.
40. J. Huang, T. Jiang, B. Han, H. Gao, Y. Chang, G. Zhao and W. Wu, *Chem. Commun.*, 2003, 1654-1655.
41. C. W. Scheeren, G. Machado, J. Dupont, P. F. P. Fichtner and S. R. Texeira, *Inorganic Chemistry*, 2003, **42**, 4738-4742.
42. S. H. Joo, J. Y. Park, J. R. Renzas, D. R. Butcher, W. Y. Huang and G. A. Somorjai, *NANO LETTERS* 2010, **10**, 2709-2713
43. N. Semagina, A. Renken and L. Kiwi-Minsker, *J. Phys. Chem. C*, 2007, **111**, 13933-13937.
44. R. A. Van Santen, *Acc. Chem. Res.*, 2009, **42**, 57-66.

Graphical abstract

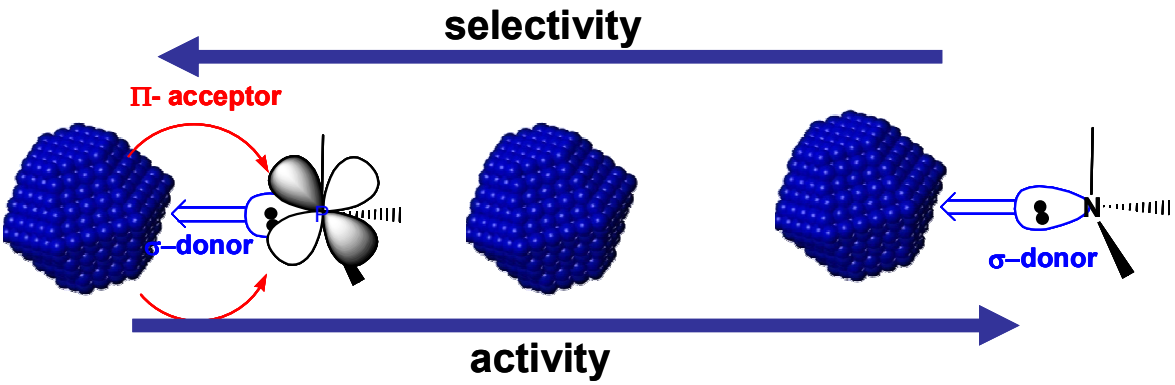

Activity and selectivity of NPs catalysts with size under 3nm could be controlled by the σ-donor π-acceptor ligands as with an homogeneous catalyst.